Implementing 1.5 millimeter Internal Diameter Columns into Analytical Workflows

Benjamin P. Libert[1,2], Justin M. Godinho[1,‡], Samuel W. Foster[2], James P. Grinias[2,*], Barry E. Boyes[1,*]

[1] Advanced Materials Technology, Inc., 3521 Silverside Road, Wilmington, DE, 19810, USA

[2] Rowan University, Department of Chemistry & Biochemistry, 201 Mullica Hill Rd., Glassboro, NJ 08028, USA

*Corresponding authors: BBoyes@Advanced-Materials-Tech.com, grinias@rowan.edu

‡Current address: CMC Analytical, GlaxoSmithKline, King of Prussia, PA 19406, USA

Abstract

The use of smaller column diameters in liquid chromatography (LC) is often associated with capillary LC. Although there are many analytical benefits gained by adapting this format, routine use continues to be challenging due to column fragility and extra column dispersion. Bridging the gap between routinely used 2.1 mm columns and capillary bore columns allows for a sequential but far from insignificant increase in performance without the need for specialized equipment associated with very low dispersion LC systems. Moreover, an incremental decrease in column internal diameter (i.d.) allows for similar mass load (avoiding column overload that may be observed in much larger decreases in i.d. without trapping) and thus an increase in measured signal. As such, 1.5 mm i.d. columns provide an alternative intermediate dimension between the more regularly used 2.1 mm i.d. columns and 1 mm i.d. columns. These columns balance an increase in sensitivity compared to 2.1 mm i.d. columns (theoretically doubling the time-domain peak area in mass sensitive detectors for the same mass load), while mitigating the efficiency losses due to extra-column dispersion effects that are commonly observed with 1.0 mm i.d. columns. Here, the use of 1.5 mm i.d. columns was applied to LC/UV analysis of small molecules and LC/MS methods for the analysis of monoclonal antibodies. With equivalent mass load on column, the 1.5 mm i.d. columns provide two-to-threefold improvement in analyte peak area signal for small molecules as well as intact, subunit, and peptide levels of antibody analysis. Peak height was also increased using the 1.5 mm i.d. column, although the scale of increase varies between

isocratic and gradient modes, likely due to differences in system dispersion effects and variation in electrospray ionization efficiency at different flow rates.

Keywords

Narrow-bore columns; Superficially porous particles; Monoclonal antibody analysis; Multi-attribute monitoring; UHPLC-MS

1. Introduction

Coupling liquid chromatography (LC) separations to electrospray ionization (ESI) sources for mass spectrometry (MS) detection without flow splitting requires columns with inner diameters (i.d.s) ≤ 2.1 mm [1]. In the regime of analytical-scale LC/MS separations, 1.0 mm i.d. columns are often used as an alternative to 2.1 mm i.d. These columns, due to their smaller i.d., require lower flow rates to achieve optimal linear velocity. Moreover, they generate higher sensitivity (more concentrated bands - *assuming identical mass load*) than can be achieved with larger diameters [2]. However, these columns often suffer from reduced chromatographic performance due to poorly packed beds [3,4] and the enhanced contribution of extra-column dispersion relative to intrinsically generated peak dispersion [5,6]. Recently, an intermediate column i.d., 1.5 mm, was shown to provide similar efficiency to 2.1 mm i.d. columns on currently available instrumentation [7]. As predicted theoretically, 1.5 mm i.d. columns exhibit optimal chromatographic performance (based on linear velocity) at half the flow rate of a 2.1 mm i.d. column. This has a twofold benefit in that it reduces solvent consumption and provides more favorable ESI conditions for desolvation and ionization for LC/MS analysis [8].

A common application for LC/MS in the biopharmaceutical industry is the characterization of monoclonal antibodies (mAbs) and measurement of various critical quality attributes (CQAs), such as post-translational modifications that can arise in the upstream and downstream processing of the mAb drug substance [9,10]. Controlling mAb drug products is critical to a mAb's biological half-life, activity, and immunogenicity, and consequently affect pre-clinical and clinical mAb efficacy [11].

Apart from using bottom-up LC/MS for mAb therapeutic process control, bottom-up approaches have been used to monitor the clearance of mAbs in animal and human serum via surrogate peptides. The pharmacokinetic study of mAbs and their surrogate peptides that are

present in pre-clinical and clinical serum samples provides guidance on how to dose mAbs efficiently and safely. However, the surrogate peptide monitoring approach continues to experience significant challenges, including low analyte sensitivity, which can negatively affect the lower limit of quantitation [12–14].

Analyte signal inherently increases with higher concentration in absorbance detection [8]. Thus, with use of a 1.5 mm i.d. column in which linear velocity is maintained at approximately half the flow rate of that with a 2.1 mm i.d. column, peaks of similar width will contain twice the concentration of analyte in the smaller diameter column if the same analyte mass is loaded onto column. This enhancement in sensitivity was explored in this study on two separate UHPLC instrument platforms. 1.5 and 2.1 mm i.d. columns were then compared by reverse phase LC/MS separations, demonstrating that an increase in MS area counts is achieved at the intact mAb, mAb subunit, and peptide levels when using the smaller diameter column under identical sample load conditions, as MS signal using ESI also increases with higher analyte concentration [15]. This enables bottom-up and top-down mAb LC/MS monitoring approaches with higher sensitivity while requiring no change in the LC/MS instrument configuration.

2. Experimental Methods

2.1 Absorbance Detection of Small Molecule Test Mixture

Uracil, phenol, 1-chloro-4-nitrobenzene, and naphthalene were obtained from MilliporeSigma (St. Louis, MO) for use in a small molecule test mixture. Comparison of detector signal using absorbance detection between the 1.5 mm i.d. and 2.1 mm i.d. columns (both 100 mm in length with Halo 2.7 µm 90 Å C18 particles) was performed under isocratic conditions of 60:40 v/v acetonitrile:water. Analysis was performed on two distinct UHPLC platforms: Nexera X2 UHPLC (Shimadzu, Columbia, MD) and Vanquish Horizon UHPLC (Thermo Fisher Scientific, Germering, Germany). The 1.5 mm i.d. columns were operated at 0.2 mL/min and the 2.1 mm i.d. columns were operated at 0.4 mL/min. For both columns on both instruments, the column oven was set to 30ºC and 0.5 µL of the sample mixture was injected. The Nexera instrument was operated with 0.075 x 300 mm tubing to connect from the injector to the column inlet, 0.060 x 700 mm tubing to connect from the column outlet to the detector flow cell, and a reported detector cell volume of 1 µL, with an overall calculated extra-column volume of 5 µL at this injection volume. The average system dispersion at these flow rates, as recorded by replacing the column with a

ZDV fitting and recording peak variance, was 1.2 μL^2. The Vanquish instrument was operated with 0.100 x 350 mm tubing to connect from the injector to the column inlet, 0.100 x 445 mm tubing to connect from the column outlet to the detector flow cell (which contained an additional 1 µL post-column cooler built into the tubing), and a reported detector cell volume of 0.8 µL, with an overall calculated extra-column volume of 8.6 µL at the same injection volume. Using the same approach as described for the Nexera, the average system dispersion observed on the Vanquish was 4.3 μL^2.

2.2 Intact mAb Sample Preparation

100 mM ammonium bicarbonate pH 8.0 (Sigma, St. Louis, MO) was prepared in deionized water obtained from an in-house source (also used for all other aqueous solutions in this study). The concentration of intact trastuzumab drug product (21mg/mL injectable formulation (Herceptin, Roche), from a pharmaceutical supplier) was confirmed spectrophotometrically (ε280nm = 225,000 M-1 cm-1). The sample was buffer exchanged into the ammonium bicarbonate using a Microcon Ultracel PL-30s centrifugal filter (MilliporeSigma, Burlington, MA) spun at 10,000 rpm until most of the drug product excipients were eliminated (3-4 replicates at 5 min each) and then checked for concentration spectrophotometrically. The buffer exchanged sample was then analyzed by LC/MS with a total on-column mAb mass of 2.8 µg.

2.3 Reduced mAb Sample Preparation

Trastuzumab drug product was denatured with 6 M guanidine hydrochloride (Thermo Fisher Scientific, Waltham, MA) in 100 mM Tris HCl at pH 7.8 (Sigma, St Louis, MO) and reduced with 12.5 mM dithiothreitol (DTT, Thermo Fisher Scientific, Waltham, MA) for 45 min at 60°C. The sample was alkylated with 20 mM iodoacetamide (Thermo Fisher Scientific, Rockford, IL) in the dark for 30 min at room temperature. Excess iodoacetamide was quenched with 20 mM DTT. The solution was diluted with 100 mM Tris pH 7.8 to 1.5 M guanidine HCl. The reduced and alkylated mAb was buffer exchanged into 0.1% TFA (Thermo Fisher Scientific, Rockford, IL) using a 5,000 MWCO Vivaspin 2 centrifuge filter (Sartorius, Bohemia, NY) spun at 4,200 rpm. For LC/MS analysis, 1.6 µg were injected on-column.

2.4 FabRICATOR (IdeS) Digestion

Trastuzumab was buffer exchanged into 100mM Tris HCl pH 7.8 using a Microcon Ultracel PL-30 centrifugal filter. FabRICATOR (Genovis, Cambridge, MA) was combined (33 units) with trastuzumab (42 µg) according to the supplier's directions (post-exchange), then incubated for 30 minutes at 37°C. The sample was diluted into 0.1%TFA and then analyzed by LC/MS with a total on-column IdeS-digested mAb mass of 2 µg.

2.5 Trypsin Digestion

Trypsin Gold MS grade (Promega, Madison, WI) was prepared at 2 µg/µL in 100 mM Tris HCl pH 7.8 and combined with reduced/alkylated trastuzumab (through the quenching and dilution steps as described in Section 2.3) in a 1:20 enzyme:protein ratio, then incubated at 37°C for 16 h. The tryptic digest was acidified with 0.5% formic acid (Sigma, St. Louis, MO) prior to LC/MS analysis of 0.3 µg of on-column digest mass.

2.6 LC/MS Analysis Conditions

Separations for the intact, reduced, and IdeS-digested samples were performed with a Shimadzu Nexera X2 UHPLC system (Columbia, MD) equipped with a Halo 2.7 µm 1000 Å diphenyl column (Advanced Materials Technology, Wilmington, DE). The column temperature was maintained at 60 °C and the flow rate was set at either 0.4 mL/min (2.1 x 150 mm), 0.2 mL/min (1.5 x 150 mm), or 0.1 mL/min (1.0 x 150 mm). Mobile phase A was composed of 0.1% difluoroacetic acid, DFA, (Sigma, St. Louis, MO) in water and mobile phase B was composed of 0.1% DFA in acetonitrile:n-propanol (1:1, both LC/MS grade from Sigma, St. Louis, MO). DFA was selected as the mobile phase additive based on its balance between chromatographic efficiency and enhanced ionization compared to formic acid and trifluoroacetic acid, respectively [16]. For the 1.0 mm i.d. column, the gradient started at 27%B and was programmed as follows: 0.01 min - 27% B, 40.0 min - 36% B, 40.5 min - 80% B, 44.5 min - 80% B, 45.0 min - 27% B, 55.0 min - 27% B. For the 1.5 mm i.d. column, the gradient started at 27%B and was programmed as follows: 0.5 min - 27% B, 40.5 min - 36% B, 41 min - 80% B, 45 min - 80% B, 45.5 min - 27% B, 50 min - 27% B. For the 2.1 mm i.d. column, the gradient started at 27%B and was programmed as follows to adjust for system dwell volume (478µL): 1.7 min - 27% B, 41.7 min - 36% B, 42.2 min - 80% B, 46.2 min - 80% B, 46.7 min - 27% B, 51.2 min - 27% B. Mass analysis was carried out on a Q Exactive HF (Thermo Fisher Scientific, San Jose, CA) operating in full scan mode. The scan range

was set to 800 to 4000 m/z at 15,000 resolution, with an automatic gain control (AGC) target of 1e6 and a max ion fill time of 250 ms. HESI II (ESI source) probe depth D was used for all columns. To minimize efficiency loss due to post-column connections [17], the column outlet was connected to the HESI source inlet with 50 µm i.d. x 600 mm length tubing (MarvelXACT, IDEX, Oak Harbor, WA).

Analysis of the tryptic digest was conducted with the same LC/MS system equipped with a Halo 2.7 µm 160 Å ES-C18 column maintained at 60 °C and operated with a flow rate of either 0.4 mL/min (2.1 x 150 mm), 0.2 mL/min (1.5 x 150 mm), or 0.1 mL/min (1.0 x 150 mm). Mobile phase A was composed of 0.1% DFA in water and mobile phase B was composed of 0.1% DFA in acetonitrile. For the 1.0 mm i.d. column, the gradient started at 2% B and was programmed as follows: 0.01 min - 2% B, 60.0 min - 50% B, 60.5 min - 80% B, 64.5 min - 80% B, 65.0 min - 2% B, 75 min - 2% B. For the 1.5 mm i.d. column, the gradient started at 2% B and was programmed as follows: 0.5 min - 2% B, 60.5 min - 50% B, 61 min - 80% B, 65 min - 80% B, 65.5 min - 2% B, 70 min - 2% B. For the 2.1 mm i.d. column, the gradient started at 2% B and was programmed as follows to adjust for system dwell volume: 1.7 min - 2% B, 61.7 min - 50% B, 62.2 min - 80% B, 66.2 min - 80% B, 66.7 min - 2% B, 71.2 min - 2% B. Here, the scan range for the MS was set to 300 to 2000 m/z at 120,000 resolution, with an AGC target of 3e6 and a max ion fill time of 50 ms. HESI II probe depth D was used for both columns here as well.

3. Results and Discussion

A recent study comparing the use of 1.5 and 2.1 mm i.d. columns described a small decrease in peak MS signal for analyses using the 1.5 mm i.d. column when the injected sample volumes were scaled to account for the smaller internal diameter compared to the 2.1 mm i.d. column [7]. This observation was attributed to the slightly wider peaks observed on 1.5 mm i.d. columns, which arise due to the larger impact of extra-column dispersion when using an identical instrument for both column types. The focus of this study is to compare the measured signal between these two column types when injecting identical sample volumes. In an initial test of a simpler mixture with absorbance detection, simply swapping the column and decreasing the flow rate by half (to maintain similar linear velocity) yielded a two-fold increase in area counts on two separate instruments (**Figure 1**). This increase arises from the same sample mass being contained within a smaller diluent volume (lower flow rate and lower inter- and intraparticle volumes

normalized for column length). Thus, the sample is less diluted on the 1.5 mm i.d. column, leading to higher concentrations and consequently higher absorbance peak area signal.

The two-fold increase in peak area signal did not necessarily lead to an equivalent increase in peak height in **Figure 1**, as observed changes in peak width between the two column diameters must be considered. In comparing the change in apparent plate count with retention factor for the four peaks shown in Figure 1 (see **Figure S1**), the expected increase in efficiency in more retained compounds was observed in both instruments [8]. However, the lower extra-column dispersion of 1.2 μL^2 on the Nexera instrument equipped with smaller i.d. connecting tubing provided closer performance between the diameters than was observed on the Vanquish instrument using standard connections that had a higher extra-column dispersion value of 4.3 μL^2. Specifically, for the naphthalene peak (k' ~ 3.3), the plate counts dropped 15% with the lower dispersion system between the 2.1 and 1.5 mm i.d. columns, while there was a 24% drop on the higher dispersion system. A van Deemter plot showing similar performance for the naphthalene peak between the two columns across a range of linear velocities is shown in **Figure S2**. In the previous study where injection volumes were scaled relative to the column diameter [7], the losses were not as significant, but this is because the extra-column effect decreases in the smaller i.d. column with the lower injection volume. In those comparisons, the measured efficiencies of the 1.5 and 2.1 mm i.d. columns began to overlap at k' values above 5, and so a similar effect would be expected here at slightly higher retention factors due to the identical injection volumes. In terms of impact on quantitative analysis, most analytical calibrations of chromatographic methods use peak area as the measured signal. However, in terms of calculating detection limits in relation to the signal above the baseline noise, the peak height is also relevant. For less retained analytes, the peak height is only slightly higher on the 1.5 mm i.d. columns due to the wider peaks. However, at k' ~ 3.3, the peak height ratio between the columns is 1.7 on the Nexera system and 1.6 on the Vanquish, thus providing a commensurate increase in sensitivity as related to peak signal. All of these calculations on isocratic performance focus specifically on 100 mm length columns packed with 2.7 µm superficially porous particles, as those were the focus on the previous and current work under these operating conditions. In previous work, the column volume of the 1.5 x 100 mm column used here was determined to be 100 µL, so the column can most effectively be used on systems with extra-column volumes less than 10 µL [7]. The 2.1 x 100 mm column volume was determined to be 173 µL, thus increasing the range of acceptable system volume to 17 µL [7]. The

effects of extra-column dispersion are related to their variance contribution relative to the column variance contribution, so factors that would lead to lower overall column volume such as smaller particle diameters and shorter column lengths would further increase the efficiency differences between the column diameters. For example, if the columns used in this comparison were decreased to 50 mm lengths, the 1.5 mm i.d. column may exceed the acceptable 10% extra-column volume limit [18] on a system with 8 µL of extra column volume, while the shorter 2.1 mm i.d. column would not. Alternatively, increasing the column volume with fully porous particle morphologies and longer column lengths would reduce the overall impact of extra-column dispersion.

Upon confirming this expected outcome using absorbance detection, the primary focus of this investigation was to measure differences in MS signal between 1.5 mm and 2.1 mm i.d. columns, specifically for mAb analysis with identical mass loads on column. When compared to the 2.1 mm i.d. column, the 1.5 mm column exhibited an approximately two-to-threefold increase in total ion current (TIC, 800 – 4000 m/z) integrated area counts for intact trastuzumab (G0/G0F average mass: 147,910 Da, **Figures 2a** and **S3a**), light chain (23,446 Da, corrected for iodoacetamide groups) and heavy chain (G0F: 50,613 Da, corrected for iodoacetamide groups) trastuzumab subunits (**Figures 2b** and **S3b**), and F_c (G0F: 25,230 Da) and F_{ab} (97,628 Da) trastuzumab subunits (**Figures 2c** and **S3c**). The deconvoluted masses were nearly identical between the column diameters, with an average Δm of 0.7 Da for all peaks. The TIC area ratio (TIC Area Ratio = TIC $Area_{1.5mm}$/TIC $Area_{2.1mm}$) for intact trastuzumab was 3.3; for light and heavy chain subunits, the ratios were 2.4 and 2.1, respectively; and for the crystallizable (F_c) and antigen-binding (F_{ab}) region subunits, the ratios were 3.1 and 2.7, respectively. Due to the similarity between the inter-column charge state envelopes observed (**Figures S4-S6**), the full scan range (800 – 4000 m/z) was used for the quantitative comparison of intact and subunit TIC chromatograms. The deconvoluted masses based on these data were the same on both column dimensions.

Considering extra-column dispersion effects for these gradient separations primarily focuses on post-column effects, as some peak focusing that reduces the broadening caused by injection and inlet connecting tubing is expected to occur [17]. Here, the outlet tubing volume was reduced to 1.2 µL to further minimize peak broadening between the column outlet and the detector. In terms of comparing the height ratio in the context of wider bands on the 1.5 mm i.d. column

due to instrument broadening under gradient conditions, the F_{ab} peak can be used for comparison as it elutes far enough into the gradient separation window that differences due to delays in the gradient timetable to account for dwell volume are minimized [19]. In this instance, the peak height ratio between the 1.5 mm i.d. and 2.1 mm i.d. columns was 2.0 for the F_{ab} peak. As with the isocratic measurements, it is slightly lower than the area ratio because of the post-column broadening effects, as the peak width at half-height for the F_{ab} fragment was 0.22 min on the 2.1 mm i.d. column and 0.27 min on the 1.5 mm i.d. column. However, this calculation is more complex when MS detection is used compared to UV absorbance detection. Enhanced area ratios above the expected value of 2 (and less than 2 for height ratios due to broadening) can likely be attributed to the lower flow rates that are used with the 1.5 mm i.d. column, as this parameter provides a more favorable desolvation condition for ESI in which ion formation can proceed via an ion evaporation-like mechanism [20,21]. In **Figure S7**, the F_{ab} on a 1.0 mm i.d. column with identical sample concentration and injection volume is shown. Again, the flow rate is reduced by half to 0.1 mL/min, but the peak height ratio is only 1.3 for the F_{ab} peak when compared to the 1.5 mm i.d. column, as its peak width at half-height is increased to 0.52 min. In this example comparison, and similarly for other peaks shown on all three columns in **Figure 2**, peak height increases moving from 2.1 mm i.d. down to 1.0 mm i.d., although the trend diminishes moving to 1.0 mm i.d. columns, partially because of post-column dispersion effects. In practice, it is likely that further optimization to enhance spray efficiency would be performed when moving from a 2.1 mm i.d. column to a 1.0 mm i.d. column, but these results demonstrate that more immediate benefits can be observed without instrument tuning simply by reducing the column diameter to 1.5 mm i.d. and decreasing the flow rate by half.

Comparing the TIC chromatograms obtained for mAb tryptic peptides when using columns with different diameters was more challenging due to the complexity of the sample mixture. The MS full scan tryptic digest chromatograms obtained using 1.5 mm i.d. and 2.1 mm i.d. columns (**Figure 3**, 300 – 2000 m/z, 1.0 mm i.d. chromatogram also shown for reference) contained numerous peptides of varying sizes, many of which were not chromatographically resolved during the analysis. To simplify the comparison, inter-column peptide area ratios were calculated using extracted ion current (XIC) chromatograms. For a single given charge state and m/z value, the XIC area ratio (XIC Area Ratio = $\text{XIC Area}_{1.5mm}/\text{XIC Area}_{2.1mm}$) provided an initial comparison. However, as charge state distribution differed between each column diameter, the peak areas of

the two most intense observed charge states were added to calculate a summed area ratio for several peptides from the trastuzumab tryptic digest. Of the peptides that exhibited multiple charge states $(M+nH)^{n+}$, the 1.5 mm i.d. column often yielded tryptic peptide species with increased relative signal intensity at higher charge state occupancies (light chain peptides **Table S1** and **Figure S8;** heavy chain peptides **Table S2** and **Figure S9**). For example, as shown in **Figure 4**, the XIC area ratio obtained for both of the heavy chain (HC) peptides HC06 and HC07 was 1.3 when Z=2 (*i.e.* $[M+2H]^{2+}$). The value increased to 8.2 and 4.9, respectively, for HC06 and HC07 when Z=3 (*i.e.* $[M+3H]^{3+}$). The summed area ratios for HC06 and HC07 were then calculated as 1.6 and 1.5, respectively. Peptide HC11 had an XIC area ratio of 0.9 at Z = 2, exhibiting similar signal on both column diameters. At the higher charge state of Z = 3, the value increased to 1.9, for an overall summed area ratio of 1.7 (**Figure 4b**). In general, the 1.5 mm i.d. column yielded peptides with 1.7-fold higher signal and modest increases in relative signal at higher charge state occupancies compared to the 2.1 mm i.d. column. As previously mentioned, differences in ESI at different flow rates likely play a role in this observation. Similarly to the larger molecules in Figure 2, the height increase observed going from 2.1 mm i.d. down to 1.5 mm i.d. is diminished when moving to 1.0 mm i.d. even with larger area, as the bands tend to broaden more here (**Figure 4**).

The value in producing peptide ions with greater intensity and at higher charge states on the 1.5 mm i.d. column may lie in the utility of performing fragmentation experiments on these higher-charge-state species. Peptide ions with $Z \geq 2$ provide structurally informative fragmentation spectra when they are collisionally-activated [22], for example, by CID or HCD. Fragmentation of peptide ions ($Z \geq 3$) by ETD also produces informative spectra [23], which can be useful in the assignment of PTM positions.

4. Conclusions

By solely reducing the column i.d. from 2.1 mm to 1.5 mm and scaling the mobile phase flow rate to the column's optimal linear mobile phase velocity, maintaining all other system settings and instrument connections the same, a two-fold increase in UV area count for a selection of small molecule standards as well as a two-fold or greater increase in TIC area counts was observed for intact mAb and mAb subunits (light chain, heavy chain, F_c, and F_{ab}). The peak heights do not necessarily scale to the same two-fold factor, as slight differences in broadening with lower volume columns due to system dispersion and benefits to ionization signal at lower flow rates both

occur. To fully realize the highest performance of 1.5 mm i.d. columns, care should be taken to minimize system dispersion, although the requirements are not as stringent as may be required for 1.0 mm i.d. columns. A two-fold average increase in the XIC peak area was also observed for tryptic peptides when the contribution from the two highest peptide charge states was used to calculate a summed area ratio. By reducing the column internal diameter to 1.5 mm, and consequently reducing the mobile phase flow rate required for operation at the optimal linear mobile phase velocity, solvent consumption decreased by half. The ease of implementing 1.5 mm columns into analytical workflows to gain a two-fold or greater increase in UV peak area signal or XIC/TIC for bottom-up and top-down LC/MS, can address the challenges of establishing sensitive methods for clinical and industrial analyses.

Acknowledgements

The authors would like to thank Tiffany Jones and Jason Lawhorn for column preparation. Andrew Harron is also thanked for insightful discussions regarding mass spectrometry ionization. This work was supported in part by the NIH/NIGMS [GM116224 to BEB]. The content is solely the responsibility of the authors and does not necessarily represent the official views, or imply endorsement, of the National Institute of Health. The Grinias Lab would like to thank Thermo Fisher Scientific for the loan of the Vanquish Horizon UHPLC system and acknowledges funding in part from the Chemical Measurement and Imaging Program in the National Science Foundation Division of Chemistry under Grant CHE-2045023.

Declaration of Competing Interest

BPL and BEB are employed by a company that manufactures some of the materials referenced in this article.

References

[1] K. Sandra, I. Vandenheede, P. Sandra, Modern chromatographic and mass spectrometric techniques for protein biopharmaceutical characterization, J. Chromatogr. A. 1335 (2014) 81–103. https://doi.org/10.1016/J.CHROMA.2013.11.057.

[2] S.R. Bakalyar, C. Phipps, B. Spruce, K. Olsen, Choosing sample volume to achieve maximum detection sensitivity and resolution with high-performance liquid chromatography columns of 1.0, 2.1 and 4.6 mm I.D., J. Chromatogr. A. 762 (1997) 167–185. https://doi.org/10.1016/S0021-9673(96)00851-5.

[3] F. Gritti, A stochastic view on column efficiency, J. Chromatogr. A. 1540 (2018) 55–67. https://doi.org/10.1016/j.chroma.2018.02.005.

[4] F. Gritti, M.F. Wahab, Understanding the science behind packing high-efficiency columns and capillaries: Facts, fundamentals, challenges, and future directions, LC-GC North Am. 36 (2018) 82–98.

[5] F. Lestremau, D. Wu, R. Szücs, Evaluation of 1.0mm i.d. column performances on ultra high pressure liquid chromatography instrumentation, J. Chromatogr. A. 1217 (2010) 4925–4933. https://doi.org/10.1016/j.chroma.2010.05.044.

[6] N. Wu, A.C. Bradley, C.J. Welch, L. Zhang, Effect of extra-column volume on practical chromatographic parameters of sub-2-m particle-packed columns in ultra-high pressure liquid chromatography, J. Sep. Sci. 35 (2012) 2018–2025. https://doi.org/10.1002/jssc.201200074.

[7] S. Fekete, A. Murisier, G.L. Losacco, J. Lawhorn, J.M. Godinho, H. Ritchie, B.E. Boyes, D. Guillarme, Using 1.5 mm internal diameter columns for optimal compatibility with current liquid chromatographic systems, J. Chromatogr. A. 1650 (2021) 462258. https://doi.org/10.1016/j.chroma.2021.462258.

[8] L.R. Snyder, J.J. Kirkland, J.W. Dolan, Introduction to Modern Liquid Chromatography, 3rd ed., John Wiley & Sons, Inc., Hoboken, NJ, USA, 2010. https://doi.org/10.1002/9780470508183.

[9] R.S. Rogers, M. Abernathy, D.D. Richardson, J.C. Rouse, J.B. Sperry, P. Swann, J. Wypych, C. Yu, L. Zang, R. Deshpande, A View on the Importance of "Multi-Attribute Method" for Measuring Purity of Biopharmaceuticals and Improving Overall Control Strategy, AAPS J. 20 (2018) 7. https://doi.org/10.1208/s12248-017-0168-3.

[10] S. Rogstad, H. Yan, X. Wang, D. Powers, K. Brorson, B. Damdinsuren, S. Lee, Multi-Attribute Method for Quality Control of Therapeutic Proteins, Anal. Chem. 91 (2019) 14170–14177. https://doi.org/10.1021/acs.analchem.9b03808.

[11] Y. Huang, R. Molden, M. Hu, H. Qiu, N. Li, Toward unbiased identification and comparative quantification of host cell protein impurities by automated iterative LC–MS/MS (HCP-AIMS) for therapeutic protein development, J. Pharm. Biomed. Anal. 200 (2021) 114069. https://doi.org/10.1016/j.jpba.2021.114069.

[12] M.T. Furlong, Z. Ouyang, S. Wu, J. Tamura, T. Olah, A. Tymiak, M. Jemal, A universal surrogate peptide to enable LC-MS/MS bioanalysis of a diversity of human monoclonal antibody and human Fc-fusion protein drug candidates in pre-clinical animal studies, Biomed. Chromatogr. 26 (2012) 1024–1032. https://doi.org/10.1002/bmc.2759.

[13] C. Gong, N. Zheng, J. Zeng, A.F. Aubry, M.E. Arnold, Post-pellet-digestion precipitation and solid phase extraction: A practical and efficient workflow to extract surrogate peptides for ultra-high performance liquid chromatography - tandem mass spectrometry bioanalysis of a therapeutic antibody in the low n, J. Chromatogr. A. 1424 (2015) 27–36. https://doi.org/10.1016/j.chroma.2015.10.049.

[14] L. Qiaozhen, Z. Xiaoyang, T. McIntosh, H. Davis, J.F. Nemeth, C. Pendley, S.L. Wu, W.S. Hancock, Development of different analysis platforms with LC-MS for pharmacokinetic studies of protein drugs, Anal. Chem. 81 (2009) 8715–8723. https://doi.org/10.1021/ac901991x.

[15] P.L. Urban, Clarifying Misconceptions about Mass and Concentration Sensitivity, J. Chem. Educ. 93 (2016) 984–987. https://doi.org/10.1021/acs.jchemed.5b00986.

[16] M.W. Dong, B.E. Boyes, Modern trends and best practices in mobile-phase selection in reversed-phase chromatography, LC-GC North Am. 36 (2018) 752–768.

[17] K. Vanderlinden, K. Broeckhoven, Y. Vanderheyden, G. Desmet, Effect of pre- and post-column band broadening on the performance of high-speed chromatography columns under isocratic and gradient conditions, J. Chromatogr. A. 1442 (2016) 73–82. https://doi.org/10.1016/j.chroma.2016.03.016.

[18] S. Fekete, I. Kohler, S. Rudaz, D. Guillarme, Importance of instrumentation for fast liquid chromatography in pharmaceutical analysis, J. Pharm. Biomed. Anal. 87 (2014) 105–119. https://doi.org/10.1016/j.jpba.2013.03.012.

[19] U.D. Neue, D.H. Marchand, L.R. Snyder, Peak compression in reversed-phase gradient elution, J. Chromatogr. A. 1111 (2006) 32–39. https://doi.org/10.1016/j.chroma.2006.01.104.

[20] J. V. Iribarne, B.A. Thomson, On the evaporation of small ions from charged droplets, J. Chem. Phys. 64 (1976) 2287–2294. https://doi.org/10.1063/1.432536.

[21] J. V. Iribarne, B.A. Thomson, Field induced ion evaporation from liquid surfaces at atmospheric pressure, J. Chem. Phys. 71 (1979) 4451–4463. https://doi.org/10.1063/1.438198.

[22] K.M. Downard, K. Biemann, The effect of charge state and the localization of charge on the collision-induced dissociation of peptide ions, J. Am. Soc. Mass Spectrom. 5 (1994) 966–975. https://doi.org/10.1016/1044-0305(94)80015-4.

[23] T.Y. Huang, S.A. McLuckey, Gas-phase chemistry of multiply charged bioions in analytical mass spectrometry, Annu. Rev. Anal. Chem. 3 (2010) 365–385. https://doi.org/10.1146/annurev.anchem.111808.073725.

Figure Captions

Figure 1. Comparison of 1.5 mm i.d. (black trace) and 2.1 mm i.d. (blue trace) columns for the separation of uracil, phenol, 1-chloro-4-nitrobenzene, and naphthalene under isocratic conditions using a Nexera X2 UHPLC instrument (top) and Vanquish Horizon UHPLC instrument (bottom).

Figure 2. The 1.0 x 150 mm (top, pink traces), 1.5 x 150 mm (middle, black traces), and 2.1 x 150 mm (bottom, blue traces) Halo 1000 Å Diphenyl 2.7 µm columns showing MS full scan [800-4000 m/z, 3-point moving average smoothing applied] chromatograms. 2.8 µg of intact trastuzumab (a), 1.6 µg reduced and alkylated trastuzumab and inset of light-chain peak (b), and 2 µg of IdES-digested trastuzumab (c) were analyzed on each column.

Figure 3. Separation of 1 µg of trastuzumab tryptic digest on 1.0 x 150 mm (top, pink) 1.5 x 150 mm (middle, black) and 2.1 x 150 mm (bottom, blue) Halo 160 Å ES-C18 2.7µm columns with MS detection (full scan [300-2000 m/z]).

Figure 4. (a). The extracted ion currents (XIC) of peptides HC06, HC07, and HC11 from a trastuzumab tryptic digest, (**Table S2**). The XIC for Z=2 (left panels) and Z=3 (right panels) for 1.0, 1.5, and 2.1 mm i.d. columns are shown. (b) Charge envelope comparison of heavy chain peptide HC11 observed using the 1.0, 1.5, and 2.1 mm i.d. columns.

Figure 1.

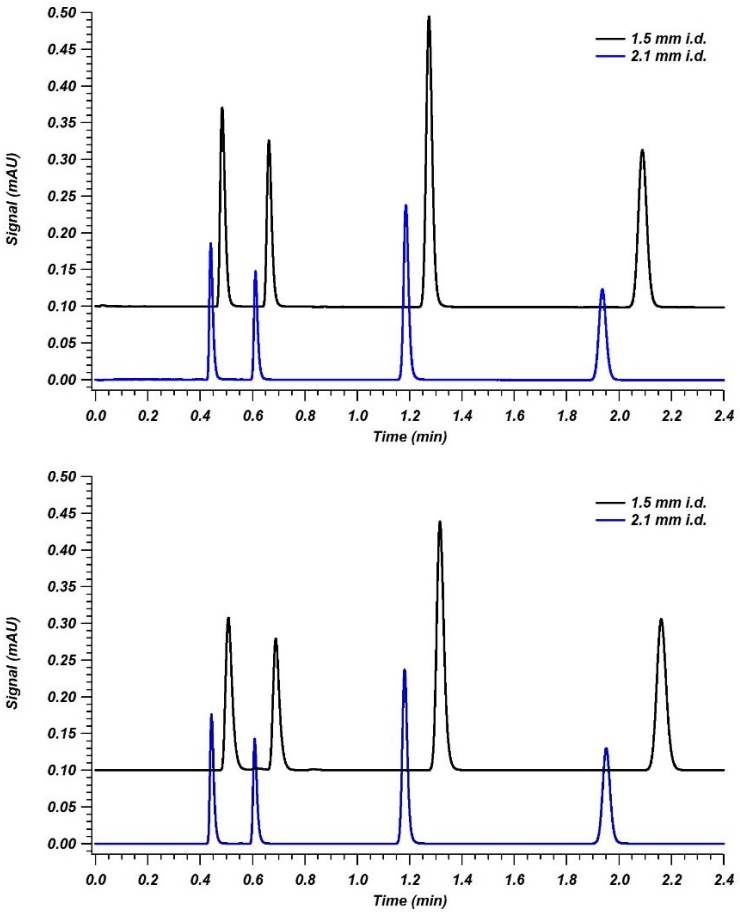

Figure 2.

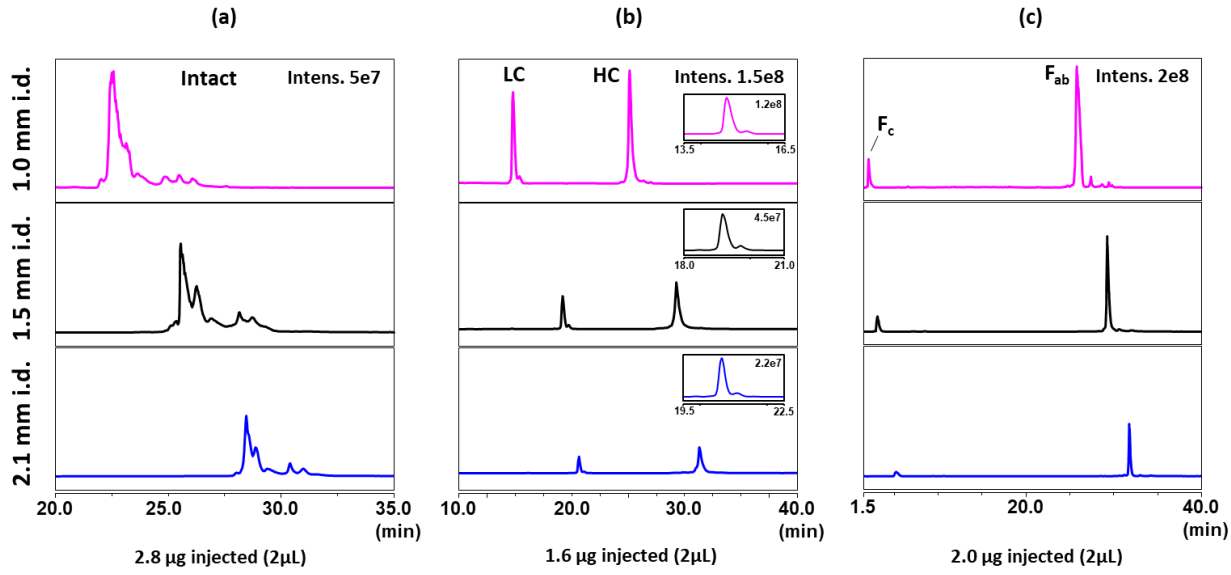

454 **Figure 3.**

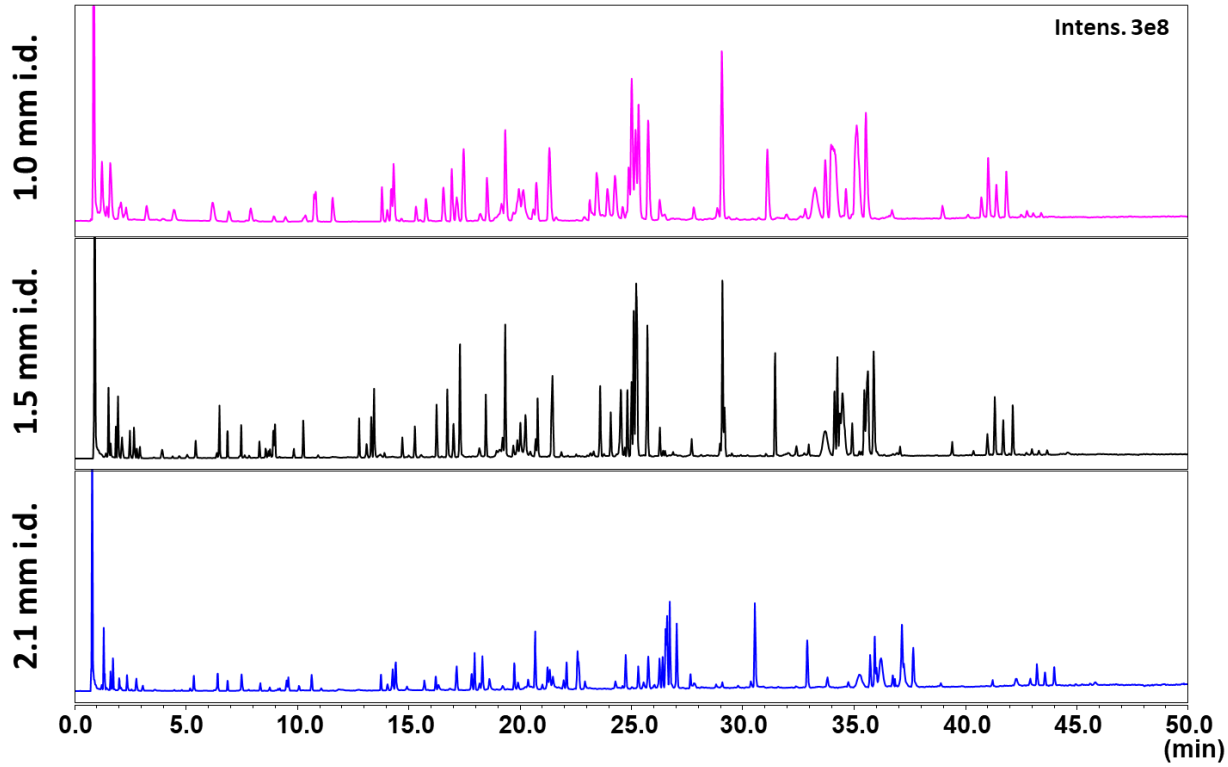

455

456

457

458 **Figure 4.**

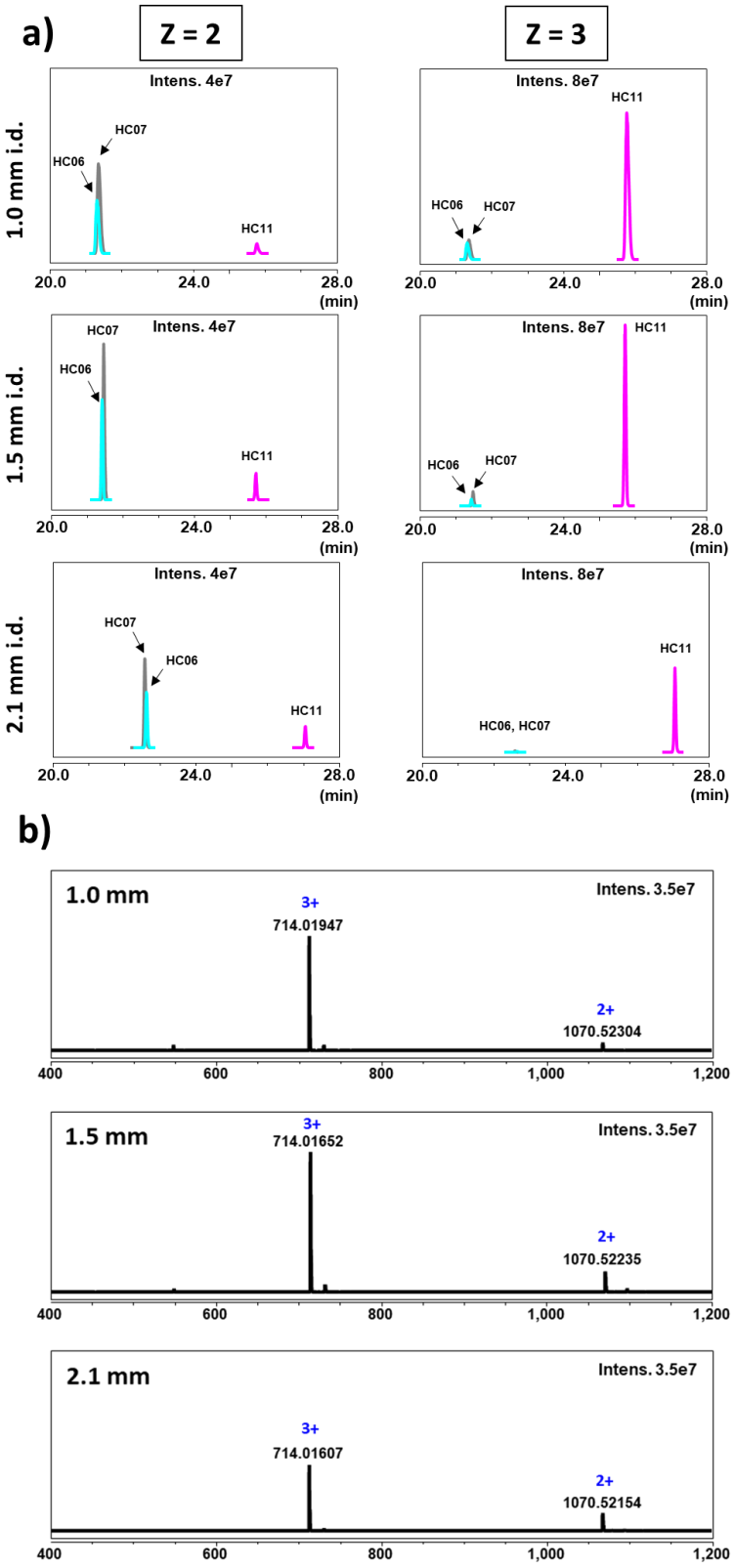

459

Implementing 1.5 mm Internal Diameter Columns into mAb Analytical Workflows

Benjamin P. Libert[1], Justin M. Godinho[1,‡], Samuel W. Foster[2], James P. Grinias[2,*], Barry E. Boyes[1,*]

[1] Advanced Materials Technology, Inc., 3521 Silverside Road, Wilmington, DE, 19810, USA

[2] Rowan University, Department of Chemistry & Biochemistry, 201 Mullica Hill Rd., Glassboro, NJ 08028, USA

*Corresponding authors: BBoyes@Advanced-Materials-Tech.com, grinias@rowan.edu

‡Current address: CMC Analytical, GlaxoSmithKline, King of Prussia, PA 19406, USA

Supporting Information

SI.1. Separation Efficiency for Isocratic Separations

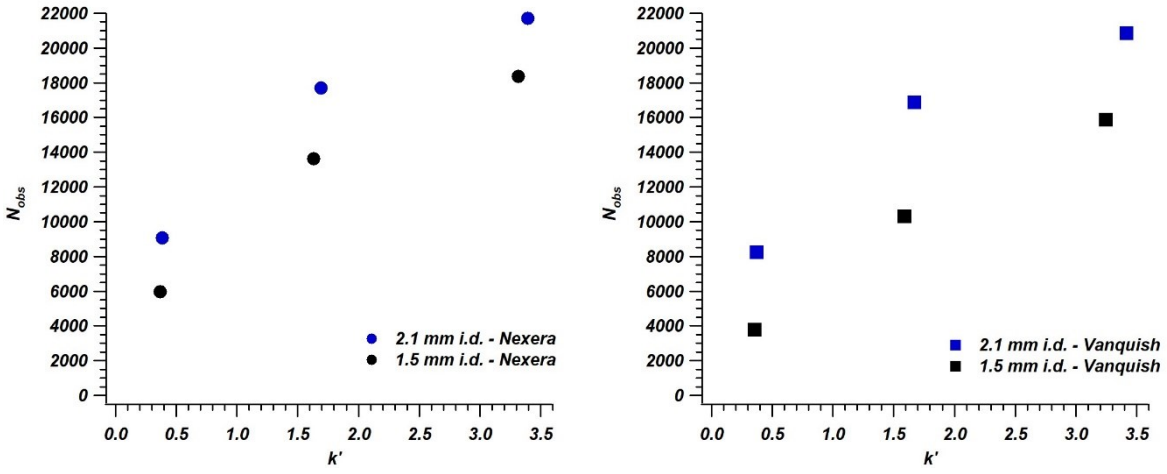

Figure S1. Relationship between observed plate count (Nobs) and retention factor (k') for separations shown in Figure 1. The left panel represents separations performed on the Nexera instrument and the right panel represents separations performed on the Vanquish instrument.

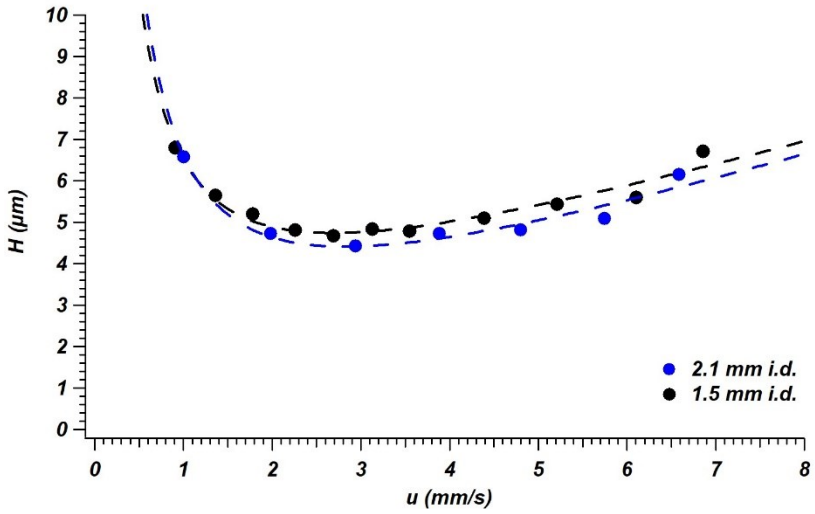

Figure S2. Comparison of van Deemter plots for naphthalene peak (k' ~ 3.3) on 1.5 mm and 2.1 mm i.d. columns on Nexera instrument. The H values are experimentally observed and not corrected for extra-column effects.

SI.2. Replicate Injections of Various Trastuzumab Samples

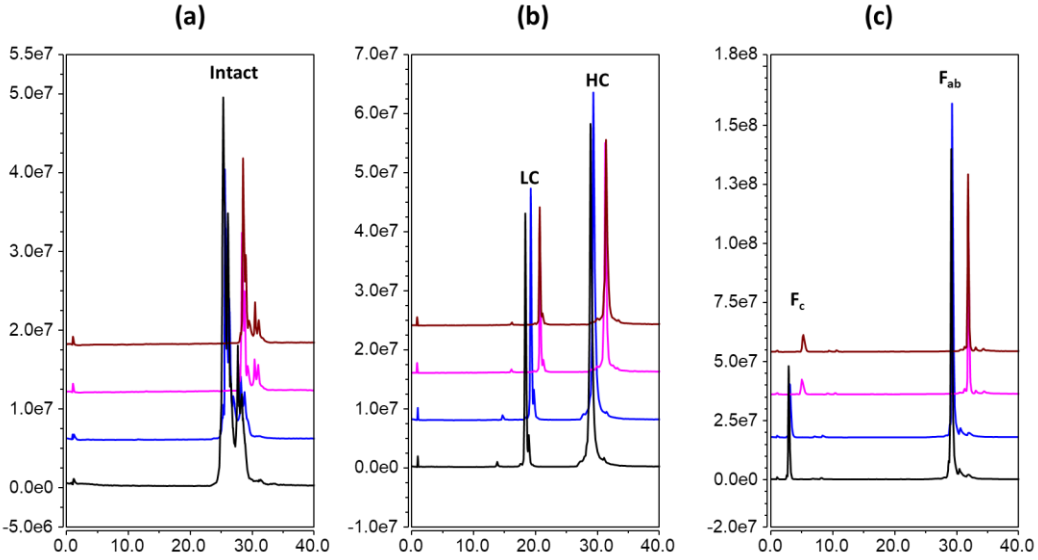

Figure S3. (a) Replicate injections of intact mAb on 1.5 mm i.d. column (blue/black) and 2.1 mm i.d. column (pink/brown), (b) replicate injections of reduced and alkylated mAb on 1.5 mm i.d. column (blue/black) and 2.1 mm i.d. column (pink/brown), and (c) replicate injections of IdeS-digested mAb on 1.5 mm i.d. column (blue/black) and 2.1 mm i.d. column (pink/brown).

SI.3. Charge State Envelope Comparison

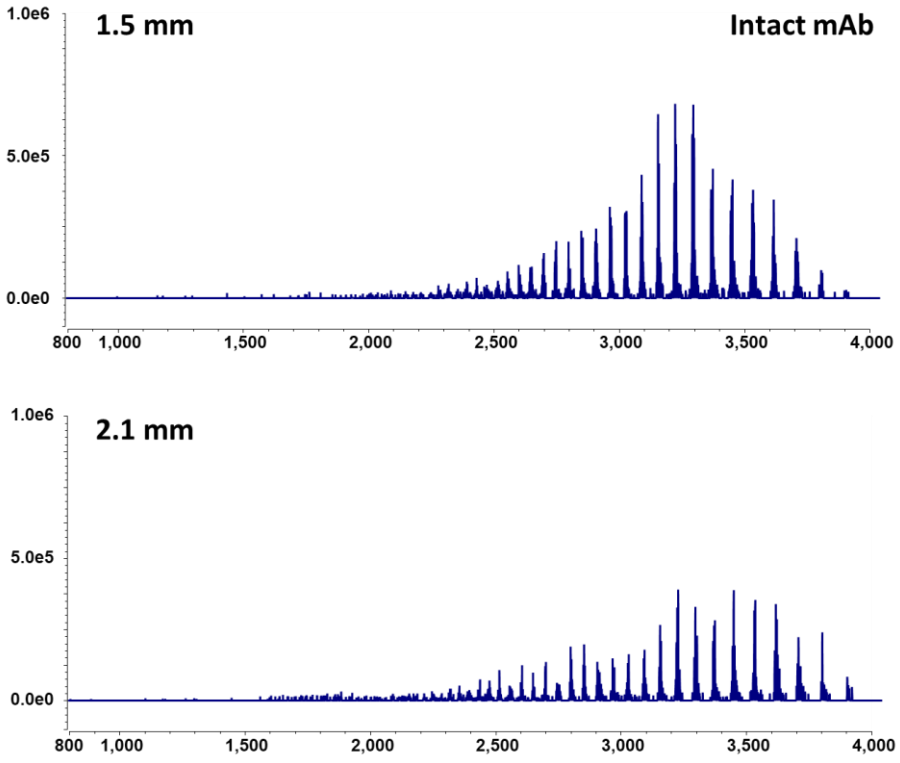

Figure S4. Comparison of charge state envelope for intact sample following elution on 1.5 mm i.d. column (top) and 2.1 mm i.d. column (bottom).

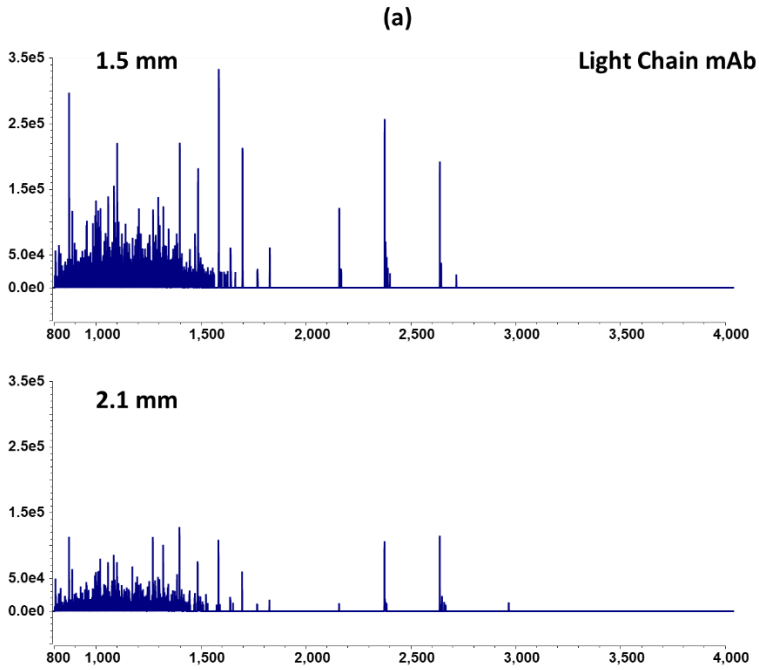

Figure S5. Comparison of charge state envelope for reduced and alkylated sample (a) light-chain and (b) heavy-chain trastuzumab following elution on 1.5 mm i.d. column and 2.1 mm i.d. column.

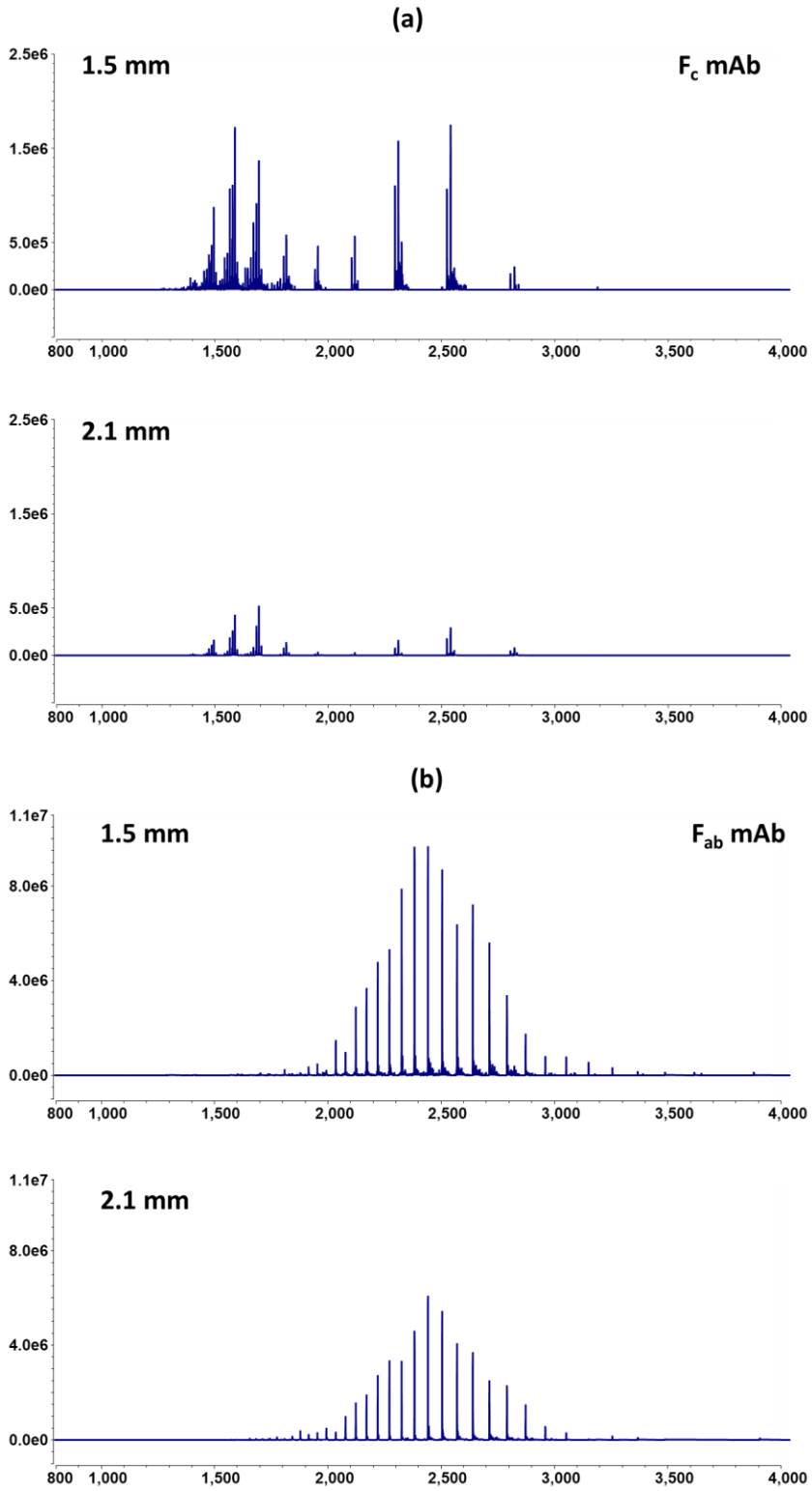

Figure S6. Comparison of charge state envelope for IdeS-digested sample with (a) F_c and (b) F_{ab} regions following elution on 1.5 mm i.d. column and 2.1 mm i.d. column.

512

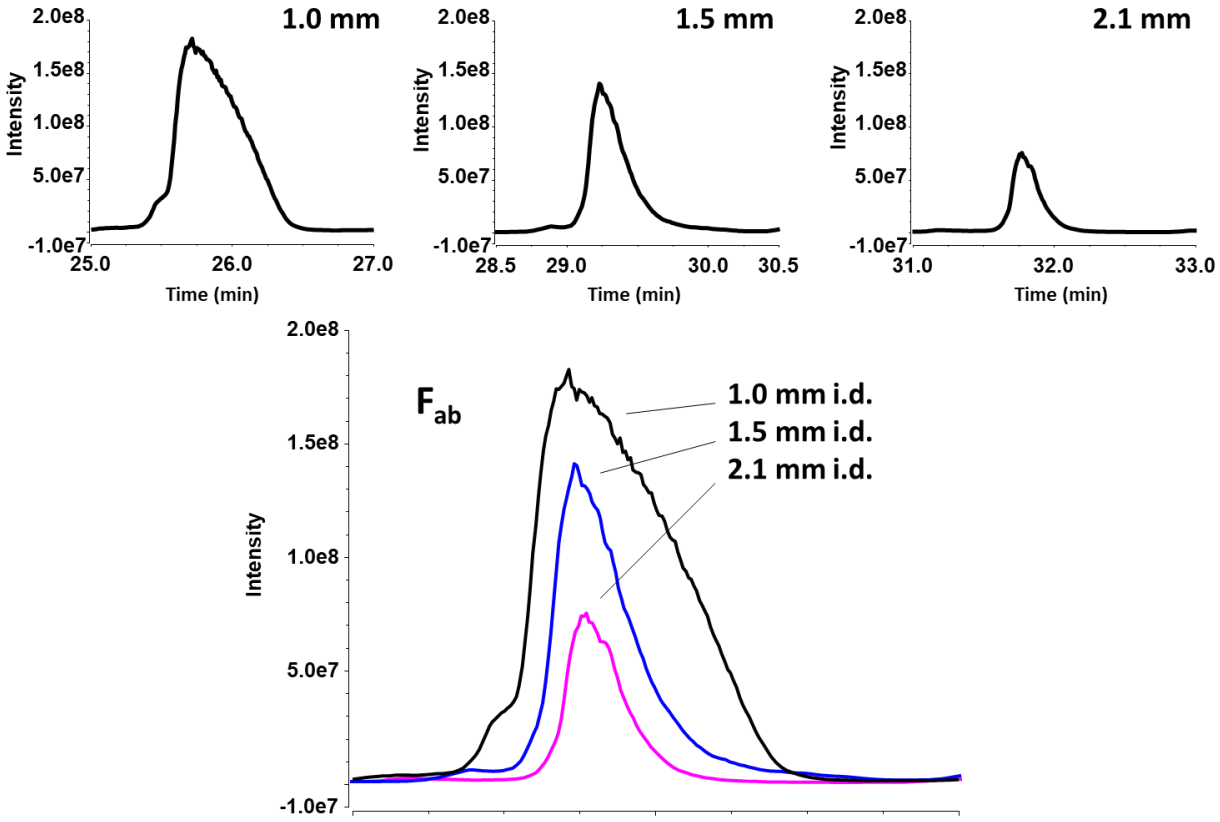

513

514

515 **Figure S7.** Total ion current chromatograms of F_{ab} region peak from trastuzumab IdeS digest on
516 Halo Diphenyl 1000 Å150 mm 2.7µm columns of 1.0, 1.5, and 2.1 mm inner diameters. The
517 bottom trace aligns the peaks to demonstrate differences in peak height and peak width.

518

SI.4. Peptide Monitoring for Trypsin-Digested Samples

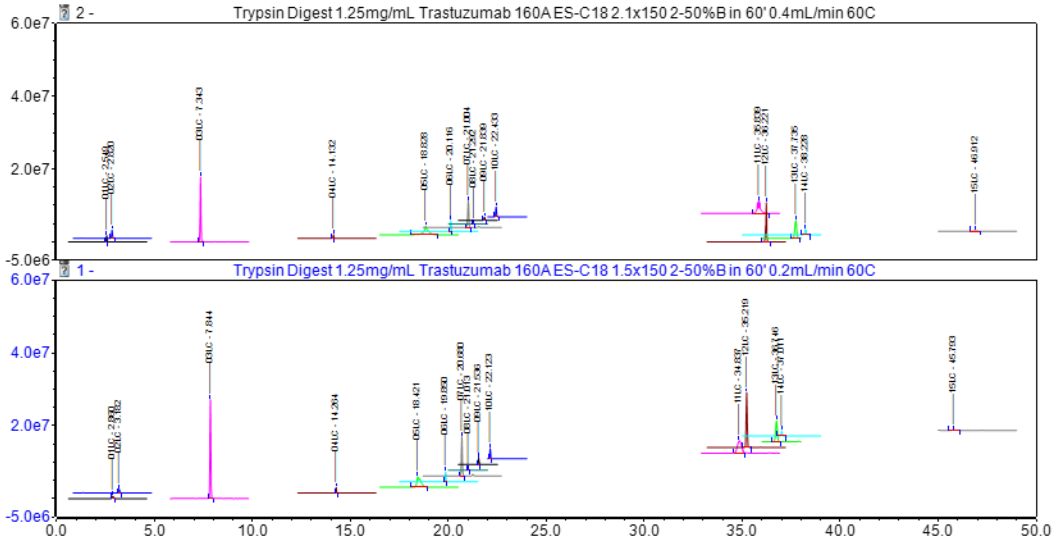

Figure S8a. Extracted ion chromatograms for light-chain peptides with a charge number of Z, identified in trypsin-digested sample elution on 1.5 mm i.d. column (bottom) and 2.1 mm i.d. column (top). Peptide sequences are found in Table 1.

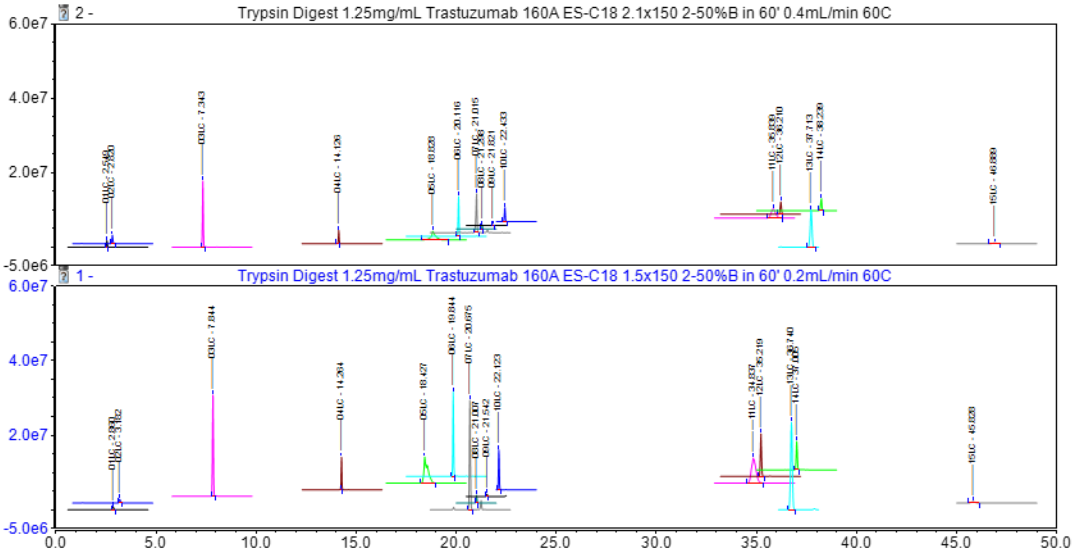

Figure S8b. Extracted ion chromatograms for light-chain peptides with a charge number of Z+1, identified in trypsin-digested sample elution on 1.5 mm i.d. column (bottom) and 2.1 mm i.d. column (top) with the following exceptions: peptides 01LC, 02LC, and 03LC exhibited only Z. Peptide sequences are found in Table 1.

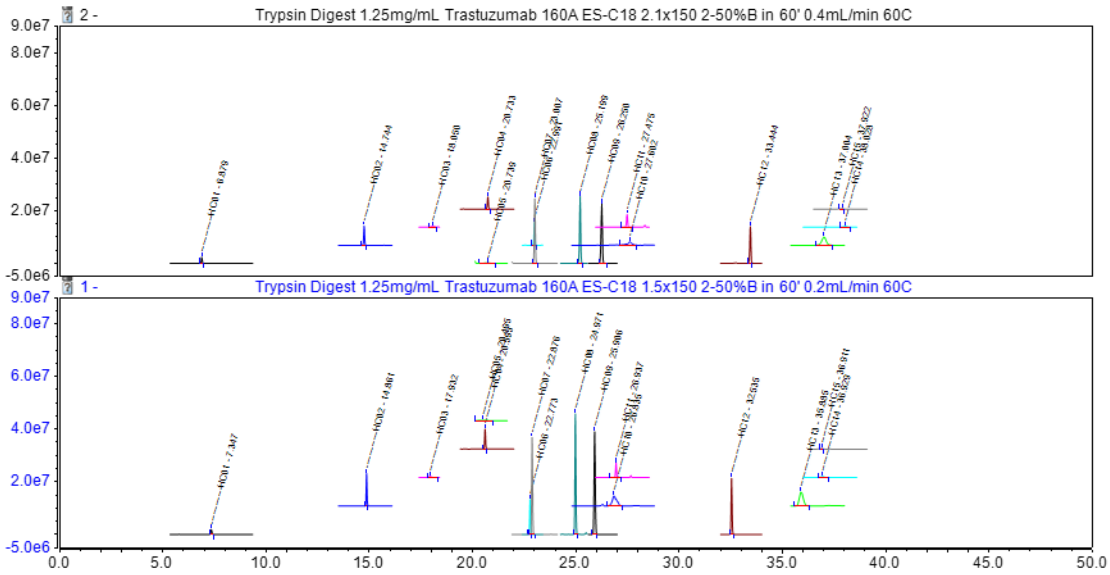

Figure S9a. Extracted ion chromatograms for heavy-chain peptides with a charge number of Z, identified in trypsin-digested sample elution on 1.5 mm i.d. column (bottom) and 2.1 mm i.d. column (top). Peptide sequences are found in Table 1.

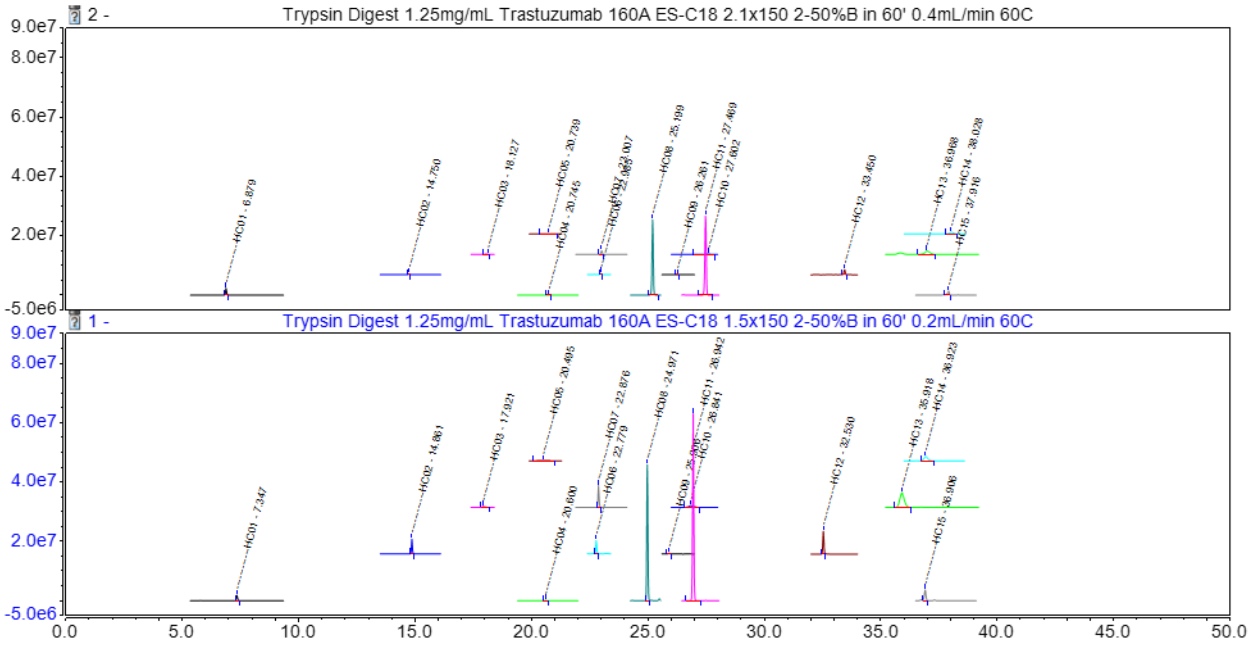

Figure S9b. Extracted ion chromatograms for heavy-chain peptides with a charge number of Z+1, identified in trypsin-digested sample elution on 1.5 mm i.d. column (bottom) and 2.1 mm i.d. column (top) with the following exceptions: peptides HC01, HC05, and HC08 exhibited only Z. Peptide sequences are found in Table 1.

543 **Table S1**. Trastuzumab Tryptic Peptides from Light Chain

544

Light Chain Tryptic Peptide	XIC $_{\text{Area Ratio}}$	Charge State (Z, Z+1)	XIC m/z (Z, Z+1)
(K)ADYEK(H)	0.7	1+	625.28, n/a
(R)FSGSR(S)	0.6	1+	553.27, n/a
(K)SFNRGEC(Carbamidomethyl)(-)	1.7	2+	435.18, n/a
(K)VDNALQSGNSQESVTEQDSK(D)	1.9	2+,3+	1068.48, 712.65
(K)HKVYAC(Carbamidomethyl)EVTHQGLSSPVTK(S)	1.8	3+,4+	714.69, 536.27
(K)VYAC(Carbamidomethyl)EVTHQGLSSPVTK(S)	1.6	2+,3+	938.47, 625.98
(R)ASQDVNTAVAWYQQKPGKAPK(L)	2.0	3+,4+	763.07, 572.55
(R)ASQDVNTAVAWYQQKPGK(A)	2.0	2+,3+	996.00, 664.32
(K)VQWKVDNALQSGNSQESVTEQDSK(D)	1.9	3+,4+	893.09, 670.06
(-)DIQMTQSPSSLSASVGDR(V)	1.9	2+,3+	939.93, 626.95
(R)TVAAPSVFIFPPSDEQLK(S)	2.3	2+,3+	973.51, 649.34
(K)LLIYSASFLYSGVPSR(F)	2.3	2+,3+	886.97, 591.65
(K)SGTASVVC(Carbamidomethyl)LLNNFYPR(E)	2.0	2+,3+	899.44, 599.96
(R)SGTDFTLTISSLQPEDFATYYC(Carbamidomethyl) QQHYTTPPTFGQGTK(V)	1.7	3+,4+	1396.62, 1047.72
(R)TVAAPSVFIFPPSDEQLKSGTASVVC(Carbamidomethyl) LLNNFYPR(E)	1.7	3+,4+	1242.29, 931.97

545

546 Z = charge number. Peptides are identified by increasing number, from top to bottom, 01LC-
547 15LC.

548 **Table S2**. Trastuzumab Tryptic Peptides from Heavy Chain

549

Peptide Sequence	XIC Area Ratio	Charge State (Z, Z+1)	XIC m/z (Z, Z+1)
(R)YADSVK(G)	0.9	1+	682.34, n/a
(R)AEDTAVYYC(Carbamidomethyl)SR(W)	1.9	2+,3+	667.78, 445.52
(K)NTAYLQMNSLR(A) oxidation	2.0	2+,3+	663.8, 442.88
(R)LSC(Carbamidomethyl)AASGFNIK(D)	1.5	2+,3+	584.30, 389.86
(R)EPQVYTLPPSR(E)	1.3	2+	643.84, n/a
[1](K)NTAYLQMNSLR(A)	1.6	2+,3+	655.84, 437.54
[2](K)STSGGTAALGC(Carbamidomethyl)LVK(D)	1.5	2+,3+	661.34, 441.22
(K)NQVSLTC(Carbamidomethyl)LVK(G)	1.6	2+	581.32, n/a
(K)GPSVFPLAPSSK(S)	1.5	2+,3+	593.83, 396.20
(R)WQQGNVFSC(Carbamidomethyl)SVMHEALHNHYTQK(S)	2.8	4+,5+	701.07, 561.05
[3](R)TPEVTC(Carbamidomethyl)VVVDVSHEDPEVK(F)	1.7	2+,3+	1070.02, 713.66
(K)TTPPVLDSDGSFFLYSK(L)	1.6	2+,3+	937.47, 625.30
(K)SC(Carbamidomethyl)DKTHTC(Carbamidomethyl)PPC (Carbamidomethyl)PAPELLGGPSVFLFPPKPK(D)	2.1	4+,5+	834.40, 667.70
(K)THTC(Carbamidomethyl)PPC(Carbamidomethyl) PAPELLGGPSVFLFPPKPK(D)	1.8	3+,4+	948.80, 711.86
(R)VVSVLTVLHQDWLNGK(E)	1.9	2+,3+	904.50, 603.30

550

551 Z = charge number. [1]HC06. [2]HC07. [3]HC11. Peptides are identified by increasing number, from
552 top to bottom, HC01-HC15.

553